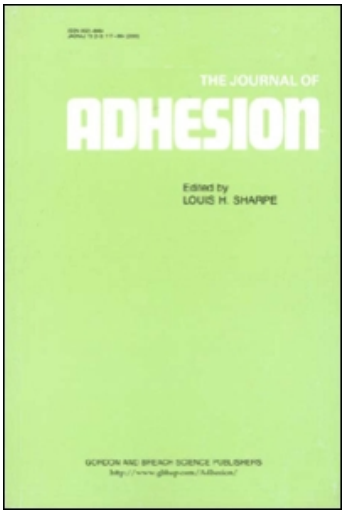

The Journal of Adhesion
Publication details, including instructions for authors and subscription information:
http://www.informaworld.com/smpp/title~content=t713453635

A Practical Criterion for Rheological Modeling of the Peeling of Pressure Sensitive Adhesives

Søren Flygenring Christensen[ab]; Stephen Carlyleflint[a]
[a] Coloplast Research, Humlebaek, Denmark [b] NKT Research Center A/S, Brondby, Denmark

To cite this Article Christensen, Søren Flygenring and Carlyleflint, Stephen(2000) 'A Practical Criterion for Rheological Modeling of the Peeling of Pressure Sensitive Adhesives', The Journal of Adhesion, 72: 2, 177 — 207
To link to this Article: DOI: 10.1080/00218460008029277
URL: http://dx.doi.org/10.1080/00218460008029277

J. Adhesion, 2000, Vol. 72, pp. 177 - 207
Reprints available directly from the publisher
Photocopying permitted by license only

A Practical Criterion for Rheological Modeling of the Peeling of Pressure Sensitive Adhesives

SØREN FLYGENRING CHRISTENSEN * and STEPHEN CARLYLE FLINT

Coloplast Research, Bakkegårdsvej 406A, DK-3050 Humlebaek, Denmark

(Received 23 June 1999; In final form 5 October 1999)

The transient extensional viscosity of non-crosslinked pressure sensitive adhesives (PSA's) and physically-crosslinked PSA's is measured and compared with theoretical predictions based on the linear viscoelastic (LVE) properties of the PSA's and the use of linear and quasi-linear constitutive equations. Based on a previously-derived expression for the relative contributions of individual relaxation modes of a polymeric material to its transient extensional viscosity, a criterion for whether large extensional deformations can be modeled on the basis of the LVE spectrum is proposed and evaluated for each PSA. The relevance to adhesion is demonstrated in peel tests, where the deformation of adhesive is quantified in images of the peel front under the assumption of uniaxial elongation and used to obtain theoretical peel forces in excellent agreement with measurements. This demonstrates the applicability of the criterion to the peeling process.

Keywords: Pressure sensitive adhesives; rheology; peel test; images

1. INTRODUCTION

The ideal tool for the formulator of pressure sensitive adhesives (PSA) is a model which predicts the adhesive performance towards a given substrate based on the chemical compositions of the adhesive and the substrate. However, adhesion depends on a complex interplay between rheology and surface properties, which are both changed when the

*Corresponding author. Present address: NKT Research Center A/S, Priorparken 878, DK-2605 Brondby, Denmark. Tel.: +45 4348 3500, Fax: +45 4363 0099, e-mail: sfc@nkt.rc.dk

chemical composition of the adhesive is altered. The effect on the surface properties still appears ambiguous, whereas the influence on the rheology, especially with respect to the linear viscoelastic (LVE) properties, has been thoroughly investigated for several classes of PSA's. The understanding gained from these investigations has provided tools for the development of adhesion models which can only be exploited if the influence of adhesive rheology on adhesion is understood.

Adhesive performance is often evaluated in peel and peel-tack tests where the quality of the adhesive bond is evaluated by measuring the resistance to debonding. Given the limitations of such tests, the bonding process cannot be quantified until the debonding process has been well characterized. During the debonding step an adhesive is stretched between a substrate and a backing material until it detaches from either or fails cohesively. Approximating the deformation of adhesive in the peel front by uniaxial elongation, the peel force is proportional to the area under the stress-strain curve as suggested by Gent and Petrich [1],

$$P = L_0 \int_1^{\lambda_{max}} \sigma(\lambda) d\lambda \tag{1}$$

where P is the peel force per width of peel strip, L_0 is the thickness of the adhesive layer, $\sigma = F_z/A_0$ is the engineering stress as function of the engineering strain, $\lambda = L/L_0$, of the elastomer. For cohesive failure the maximum strain attained equals the strain at break. In the case of adhesive failure the maximum strain attained equals the strain at detachment. For evaluation of the integral they advocated the use of stress-strain data obtained in uniaxial elongation of elastomer at constant strain rate,

$$\dot{\varepsilon}_0 = v/L_0 \tag{2}$$

where v is the peel rate and L_0 is the adhesive layer thickness. The model was experimentally evaluated and reasonable agreement between theoretical and measured peel force values in cases of cohesive as well as adhesive failure was reported. In a refinement of the method, Verdier *et al.*, combined experimental transient extensional viscosity data with model predictions based on a Lodge model and evaluated

the integral (1) at constant strain rate in accordance with Eq. (2) over a wide range of peel rates [2, 3].

Connelly, Parsons, and Pearson evaluated the integral (1) for T-peeling of a polyester hot-melt adhesive in the cohesive failure mode, employing stress-strain data from uniaxial elongation at decreasing strain rate to simulate better the actual strain history experienced during the peeling process [4]. This illustrates the problem with the integral (1), namely, that it depends on an arbitrary choice of the strain rate profile. Gupta addressed this issue by suggesting a more general expression for P in the case of cohesive failure [5]:

$$P = \int_0^{x_b} \sigma(x)dx \tag{3}$$

where $\sigma(x)$ is the stress distribution at the adhesive/substrate interface across the peel front, x is the horizontal position in the peel front, and x_b is the position at which the adhesive ruptures cohesively. Gupta derived the integral (3) under an explicit assumption of cohesive failure within the adhesive bulk but, in fact, the derivation does not depend on this assumption. In the case of adhesive failure x_b is simply the position at which the adhesive detaches from the substrate. Christensen *et al.*, quantified the deformation of adhesive in images of the peel front and obtained near quantitative predictions of peel force with the use of Eq. (3) for a PSA exhibiting adhesive failure [6].

For a 90° peel geometry with a horizontally-oriented substrate surface, Eq. (3) can be derived from a simple one-dimensional force balance: Assuming steady state in the Eulerian sense during a 90° peel test, the same force must act across every horizontal plane at all times. In a horizontal cross-section of the peeled adhesive strip far away from the peel front, the bulk adhesive has relaxed after detachment from the substrate and the peel force is transferred in the vertical direction by the backing material. Furthermore, for the horizontal plane coinciding with the adhesive/substrate interface the effective vertical force is transferred by the adhesive in the peel front and is given by Eq. (3). According to this derivation, both the elastic and the viscous deformation of the adhesive contribute to the total peel force, *i.e.*, the elastically-stored energy is not regained when the adhesive retracts after detachment from the substrate.

In disagreement with the models and considerations above, Gent and Hamed stated that only the viscous deformation of elastomer contributes to the total peel force and proposed a modification of Eq. (1) in accordance with this statement [7–10],

$$P = l_0 \int_1^{\lambda_{max}} \sigma_L(\lambda) - l_0 \int_1^{\lambda_{max}} \sigma_U(\lambda) d\lambda \tag{4}$$

where subscripts "L" and "U" refer to the loading and unloading in a cyclic tensile test. The authors did not suggest any mechanism by which the energy spent in elastic deformation could be regained after the adhesive detaches from the substrate or breaks cohesively. However, good agreement between measured and theoretical peel force values based on cyclic stress-strain data and the use of Eq. (4) were reported. For purely viscous fluids, Eqs. (1) and (4) predict the same value of P, but such materials do not posses PSA properties. Anyway, the idea that the energy dissipated viscously (loss portion) is the sole contribution to the peel force has been adopted by several researchers and has had considerable influence on the development of approximate models for correlation of adhesive performance of PSA's to their LVE properties. This subject is further treated below.

Because rheological properties have been identified as key parameters in the performance of PSA's and because oscillatory shear testing, also termed dynamic mechanical analysis (DMA), is the most popular method for rheological characterization of PSA's, a lot of effort has been devoted to the development of approximate models for correlation of adhesive performance to the storage and loss moduli, G' and G'', and their ratio, $\tan\delta = G''/G'$. The lowest $\tan\delta$ peak temperature, which can be obtained from temperature sweeps, is a very popular parameter in this field and is often regarded as an approximate measure of the glass transition temperature, T_g.

Various relations between DMA data and peel performance have been proposed. Most of these are based on the same basic principle, that since the peeling process involves high deformation rates of the adhesive, the debonding process should be correlated to the LVE response of the adhesive measured at high frequency [11–13]. The main point of disagreement seems to be whether debonding should be correlated to the elastic, G', or to the viscous, G'', component of the

complex modulus, G^*, or to tan δ. The discussion can be traced back to the discrepancy between the perceptions leading to Eqs. (1) and (4) above. Those researchers who prefer Eq. (4) only consider G'' or, alternatively, tan δ, and those who prefer Eq. (1) use G' as the key parameter. In order to be fully consistent with Eq. (1) both the elastic and the viscous contributions should be considered but, since most PSA's are rubbery, with $G' > G''$ over a broad range of frequencies, the contribution from G'' is often ignored.

For correlation of the peel response of a PSA to its LVE properties Wong suggested the use of a DMA test frequency, the so-called debonding frequency, ω_D, proportional to the peel rate over a characteristic length, λ, measured in images of the peel front [14]. Tse later proposed a more easily applied expression for ω_D, replacing λ with the adhesive layer thickness, L_0 [15–17],

$$\omega_D \cong 2\pi v/L_0 \tag{5}$$

which prescribes the use of frequencies of the order 10^2–10^3 rad/s for the debonding conditions in typical industrial tests. This relation follows from Eq. (2) by assuming that the most relevant oscillatory shear test frequency for correlation of LVE data to the extensional properties of a PSA material is proportional to the strain rate by a factor of 2π; a reasonable assumption for purely viscous fluids but not for viscoelastic materials such as typical PSA's. However, for any series of PSA's of varying T_g one almost inevitably finds strong correlations between adhesive performance and the LVE properties measured at high frequency such as ω_D in Eq. (5), because the high frequency LVE response, as well as the adhesive performance, depend strongly on T_g. Experimental findings by Dale, Paster, and Haynes [18] demonstrate that for a series of PSA's of *constant* T_g it is the low frequency LVE response which is the more relevant for correlation of DMA data to peel performance. For a series of solvent-based acrylic PSA's with $T_g \cong 5°C$ (tan δ peak position) of varying cross-link density they found that the best correlation between peel force and DMA data was obtained with the use of $\omega_D = 1$ Hz at 127°C. According to the WLF equation for the shift factor [19] this is equivalent to $\omega_D \cong 10^{-7}$ rad/s at 23°C – a value that is orders of magnitude lower than suggested above. At this low frequency the network structure is probed.

Bridging the gap, Christensen and McKinley [20] demonstrated that, in fact, a wide range of DMA test frequencies are relevant for correlation of DMA data to peel performance and found that the relative contributions, f_i, from discrete relaxation modes to the total peel force can be approximated by

$$f_i = \frac{\eta_i(1 - \exp(-t_b/\lambda_i))}{\sum_{i=1}^{N} \eta_i(1 - \exp(-t_b/\lambda_i))}, \quad i = 1, 2, \ldots, N \tag{6}$$

where η_i, and λ_i are the viscosity and time constant, respectively, of relaxation mode i, N is the total number of relaxation modes used to describe the adhesive, and t_b is the residence time of adhesive in the peel front. Each relaxation mode can then be represented by a specific DMA test frequency

$$\omega_i = 1/\lambda_i \tag{7}$$

This paper addresses the general question of whether uniaxial elongation of a polymeric material beyond the linear range can be modeled on the basis of its LVE spectrum and how Eqs. (6) and (7) can be used to answer this question. The concept is then applied to the peeling of PSA's.

2. EXPERIMENTAL

2.1. Materials

Five PSA's were studied: A previously-described model adhesive, A1 [6, 20], two commercial hydrocolloid skin adhesives, A2 and A3, and the unfilled counterparts or matrices of A2 and A3 termed M2 and M3 respectively. A2 is used to attach ostomy bags to the skin and A3 is a wound-care adhesive. On the macroscopic level, the commercial skin adhesives have a two-phase morphology consisting of a dispersed hydrophilic polymer (hydrocolloids) in a hydrophobic elastomeric matrix. The hydrocolloids constitute 45% and 40% of the total weight of A2 and A3, respectively. M2 consists of polyisobutylene (PIB) and an aliphatic tackifying resin, and M3 consists of polystyrene-polyisoprene-

polystyrene (SIS) tri-block copolymer tackified with a mid-block compatible resin. M3 is believed to be microphase separated in the following way: The polystyrene endblocks form dispersed domains which act as physical crosslinks and give the material its rubbery properties. M3 is softened with a plasticiser which enters both the continuous elastomeric phase and the dispersed endblock domains.

Polycarbonate (PC), poly(vinylidene fluoride) (PVDF), and stainless steel (SS) were used as substrate materials. Injection-moulded PC and PVDF plates of well-defined roughness were obtained with the use of special moulds, made rough by electric sparks. Well-defined roughness of the SS plates was also obtained by electric sparks, in the hope that this would lead to the same surface structure of all substrates independent of material. Smooth plates of all three materials were used as well.

2.2. Surface Characterization of Substrate Materials

Substrate roughness was measured with a Taylor-Hobson Surtronic 3+ device which draws a pick-up across the surface along a straight line, recording the roughness profile in that particular direction. From this profile the software computes the average peak height, r_a. On the smooth substrates, droplet contact angles of a series of formamide/2-ethoxyethanol mixtures (tantech, ASTM-D 2578-67) of varying surface tension and with purified water (18 MΩ) were measured with video equipment (VCA2500, AST Products).

The surface characteristics are summarized in Table I. As expected, the three levels of r_a are nearly identical for the PC and the PVDF plates because they were moulded in the very same moulds. The range of r_a values for the stainless steel (SS) plates is a little more narrow. The surface profiles for the roughest substrate of each material are compared in Figure 1. As intended, the surface profiles are indeed similar in nature. The slightly lower value of r_a for the SS-7 plate is recognized in Figure 1, and a closer look at the figure further reveals that the average horizontal distance between peaks, r_{sm}, is somewhat lower for the SS-7 plate than for the polymeric plates.

The critical surface tension, γ_c, of the smooth steel plates (SS-0) is much lower than expected, and the contact angle with water, θ_w, is surprisingly high. Therefore, one SS-0 plate was analysed by X-ray

TABLE I Surface properties of the peel substrates

Substrate	r_a[a] (μm)	*S.D.*[b]	θ_w[c] (*deg.*)	γ_c[d] (*dyn/cm*)
PC-0	< 0.1	–	91	18
PC-2	1.95	0.10	–	–
PC-8	8.24	0.72	–	–
PVDF-0	0.1	0.02	74	30
PVDF-3	2.5	0.3	–	–
PVDF-9	9.1	0.3	–	–
SS-0	0.17	0.05	97	28
SS-4	4.2	0.4	–	–
SS-5	4.9	0.5	–	–
SS-7	7.0	0.6	–	–

[a] Average peak height.
[b] Standard deviation of the four measurements of r_a.
[c] Contact angle with water.
[d] Critical surface tension – determined from Zisman plots.

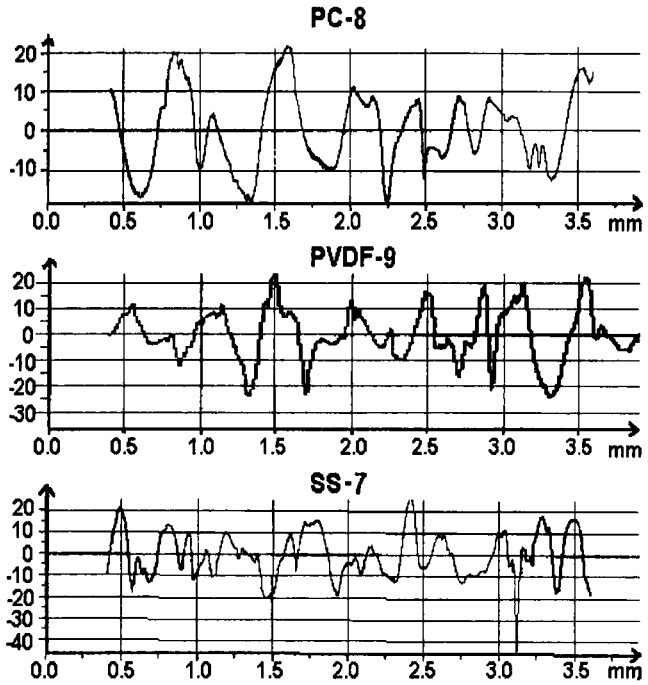

FIGURE 1 Substrate surface profiles for the roughest substrate of each substrate material.

photon spectroscopy (XPS) which revealed an elementary surface composition of 54.6% C, 38.8% O, 4.5% Fe, and 2.1% Cr. The very low content of Fe and the high content of carbon at the surface probably account for the unexpected values of γ_c and θ_w. Possibly the surface composition of the roughened plates was different due to the treatment with electric sparks.

2.3. Peel Tests

Test samples were prepared by applying a backing tape (Tesa tape 4651, Beiersdorf AG) onto a 25 mm wide and 1.0 mm thick adhesive strip. The resulting laminate was then cut into slim strips only 2.0 mm wide. Three such strips were applied manually to each test substrate and passed over by a 2 kg roll at 10 mm/s, then left to equilibrate for 24 hours at 60°C. After conditioning for one hour at 23°C and 50% relative humidity the peel force was measured at the same environmental conditions and a peel rate of 304 mm/min with the use of a peel stage mounted in a load frame (Instron 5564). The total length of adhesive peeled in each test was 30 mm for the PC and PVDF plates and 90 mm for the SS plates.

2.4. Rheological Characterization

The linear viscoelastic (LVE) properties of A1 were measured in oscillatory shear, also termed dynamic mechanical analysis (DMA), in a Rheometrics RMS 800 instrument, using a 25 mm diameter, parallel-plate geometry at 5% strain. The LVE properties of M2 and M3 were measured in the same way in a Rheometrics ARES instrument. The LVE properties of A2 and A3 were measured in the ARES instrument with the use of serrated plates to ensure no slip of the less sticky PSA's and at lower strains (0.2% for A2 and 0.5% for A3) due to more narrow linear ranges of the filled materials. The transient extensional viscosity was measured in a filament-stretching instrument. The instrument and the method has been previously described [20]. Additional measurements of the extensional properties of A3 were carried out in an Instron 5564 load frame.

3. RESULTS AND DISCUSSION

3.1. Linear Viscoelastic Properties

Figures 2 to 6 show the linear viscoelastic (LVE) properties of A1, M2, A2, M3, and A3, respectively, shifted to 23°C by time-temperature superposition of data sets obtained in frequency sweeps from 10^{-2}–10^{2} rad/s at various temperatures. The solid lines represent best fits to experimental data of discrete multimode relaxation spectra which will subsequently be used to model the material response in uniaxial elongation in Section 3.2 below. Al is shear thinning and the complex viscosity, η^*, can be approximately described by a power law expression in the frequency range 10^{-2}–10^{2} rad/s as indicated by the linearity of the log–log graph representing η^* in Figure 2. At frequencies below 10^{-2} rad/s, η^* plateaus at the zero shear viscosity,

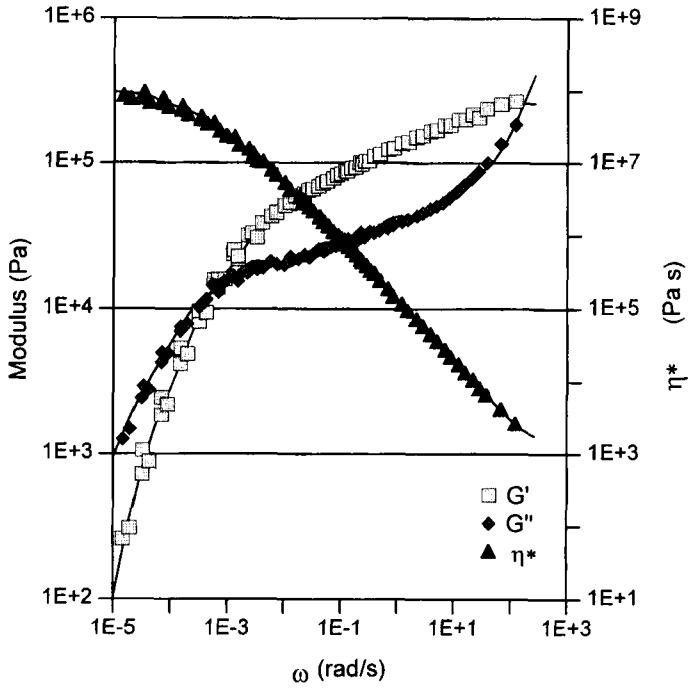

FIGURE 2 Linear viscoelastic properties of A1 shifted to 23°C. The solid lines represent the best fit of a discrete relaxation spectrum.

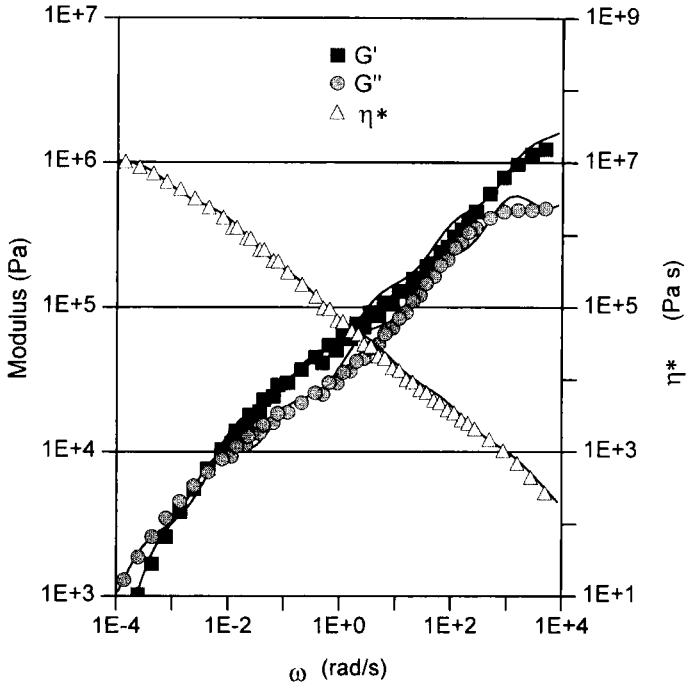

FIGURE 3 As Figure 2 but for M2.

$\eta_0 \cong 10^8$ Pa s. Over a wide range of frequencies Al is rubbery with $G' > G''$. M2 is shear thinning in the full frequency range examined, but η^* does not quite obey a power law expression. Below 10^{-3} rad/s, η^* tends to level off, hinting at a zero shear viscosity of the order $3 \cdot 10^7$ Pa s. Adding hydrocolloids to this matrix changes the LVE properties considerably, especially at low frequencies, where the loss and storage moduli, G'' and G', are increased by one and two orders of magnitude, respectively. The crossover frequency is shifted from about $7 \cdot 10^{-3}$ rad/s to less than 10^{-4} rad/s, and the tendency for the complex viscosity to level off at the lowest frequencies has vanished. This means that addition of hydrocolloids to the matrix material has introduced a higher time constant, which may stem from the interface between the matrix and the hydrocolloids, from the rheological response of the hydrocolloids themselves, or a combination of both.

At frequencies above 10^2 rad/s, the LVE spectrum of M3 in Figure 5 resembles that of M2 except for a slight vertical shift, but below that

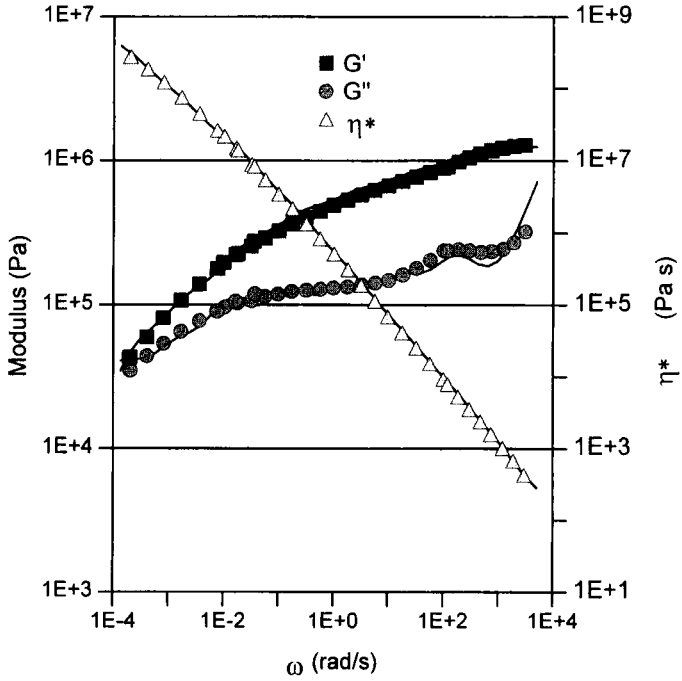

FIGURE 4 As Figure 2 but for A2.

frequency the spectra deviate strongly. The moduli of M2 drop steeply with decreasing frequency, as is characteristic of polymer melts, whereas those of M3 level off due to the physical cross-links constituted by the styrene endblocks of the tri-block copolymer. The LVE spectrum of A3 (M3 + 40%w/w hydrocolloids) in Figure 6 is similar to that of A2 at high frequency, but differs at low frequency as the fingerprint of physical cross-links is still clearly recognizable.

3.2. Transient Extensional Viscosity

Figures 7 to 12 show plots of the transient extensional viscosity, $\bar{\eta}_E^+$, of A1, M2, A2, M3, and A3, respectively, comparing measured values with model predictions based on the multimode spectra represented by solid lines in Figures 2 to 6 and the use of three viscoelastic models (given in the Appendix): the generalized linear Maxwell model (linear),

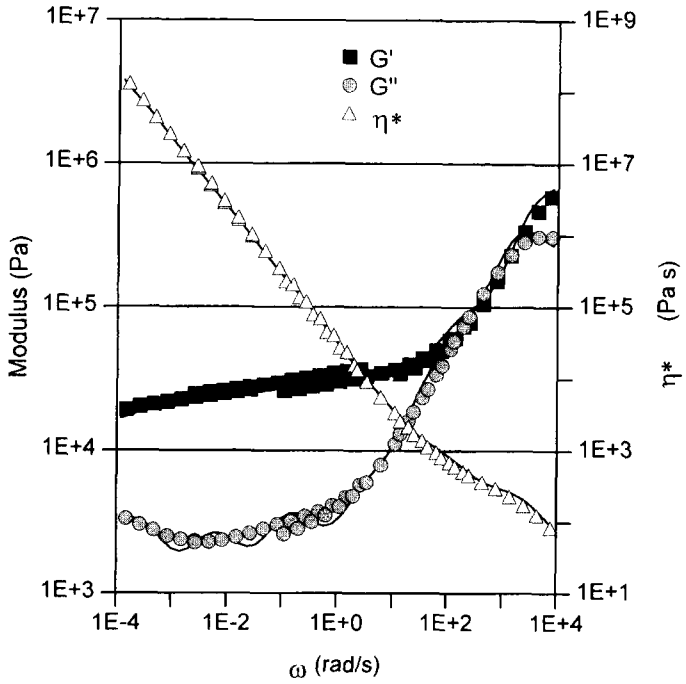

FIGURE 5 As Figure 2 but for M3.

the generalized upper-convected Maxwell model (quasi-linear), and the generalized Giesekus model (non-linear). At short times, the non-linear model reduces to the quasi-linear model but predicts less strain hardening at longer times depending on the magnitude of the mobility factors, α_i, of each relaxation mode. At a strain rate of $0.88\,s^{-1}$ the transient extensional viscosity of A1 increases according to the quasi-linear predictions at $t < 0.5$ seconds, whereafter significant deviation from the linear as well as the quasi-linear predictions is observed. It is significant, however, that the response remains within the bounds given by the linear and the quasi-linear models. To enable accurate modeling of the tensile stress growth of A1 during peeling, in Section 3.5 below the non-linear model was applied, and the mobility factors, α_i, of each relaxation mode were adjusted to obtain a better fit to the observed experimental response as shown in Figure 7. At a strain rate of $0.51\,s^{-1}$ (Fig. 8) the transient extensional viscosity of M2

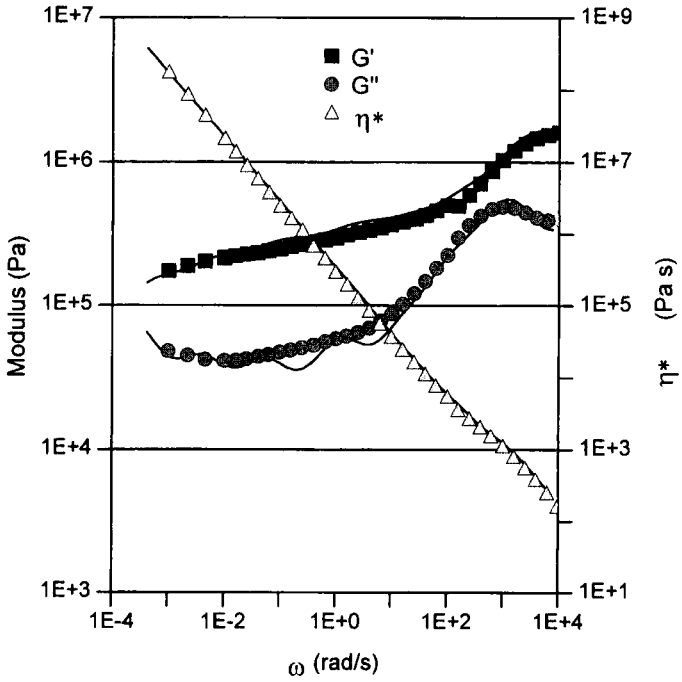

FIGURE 6 As Figure 2 but for A3.

follows the same trends as were observed for A1. Again, it is noticeable that the response remains within the bounds given by the linear and quasi-linear models. As can be seen in Figure 9 the main effects on the extensional response of loading M2 with hydrocolloid particles (to produce A2) are an increase in the transient extensional viscosity at low strains and a reduction in the strain hardening at higher strains. The linear model fits the experimental data at high and low times but deviates up to a factor of three at intermediate times. At higher strain rates (Fig. 10) the quasi-linear model exhibits excellent fit to the measured values at times $t < 0.23$ s, where the transient extensional viscosity abruptly drops about 15%. From then on the linear predictions fit the measured values quite well. Considering the complex morphology of A2, with a dispersed phase taking up nearly half of the total volume, the linear model all in all does a surprisingly good job. The abrupt drop in extensional viscosity may be due to debonding of the polymer matrix from the hydrocolloid particles, or it may be

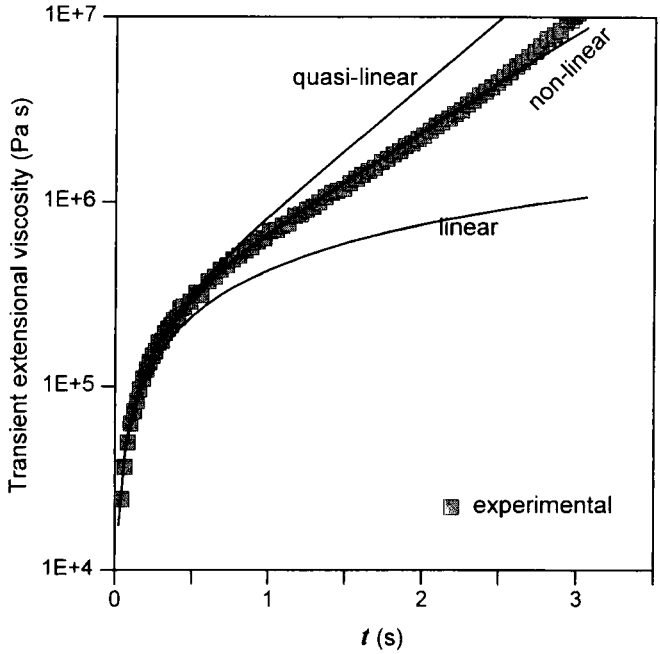

FIGURE 7 Transient extensional viscosity, $\bar{\eta}_E^+$, of A1 measured at a strain rate $\dot{\varepsilon}_0 = 0.88\,s^{-1}$ at 23°C. The experimental data are compared with theoretical predictions based on the discrete relaxation spectrum represented by solid lines in Figure 2 and the use of three viscoelastic models: The generalized linear Maxwell model (linear), the generalized upper-convected Maxwell model (quasi-linear), and the generalized Giesekus model (non-linear).

correlated to a possible yield stress of the dispersed phase. Why there is no trace of a similar drop at low strain rate is not understood.

It is clear from Figure 11 that for M3 the observed extensional response disagrees with the linear as well as the quasi-linear model predictions based on the LVE spectrum. The material response resembles that predicted by the quasi-linear model but remains far above the quasi-linear model prediction based on the LVE spectrum throughout the experiment, indicating that the transient extensional response of a strongly crosslinked material such as M3 may not be quantitatively correlated to the LVE properties. The same trend is recognized in Figure 12 showing a similar plot for the skin adhesive, A3. Even at early times the observed response disagrees with both model predictions.

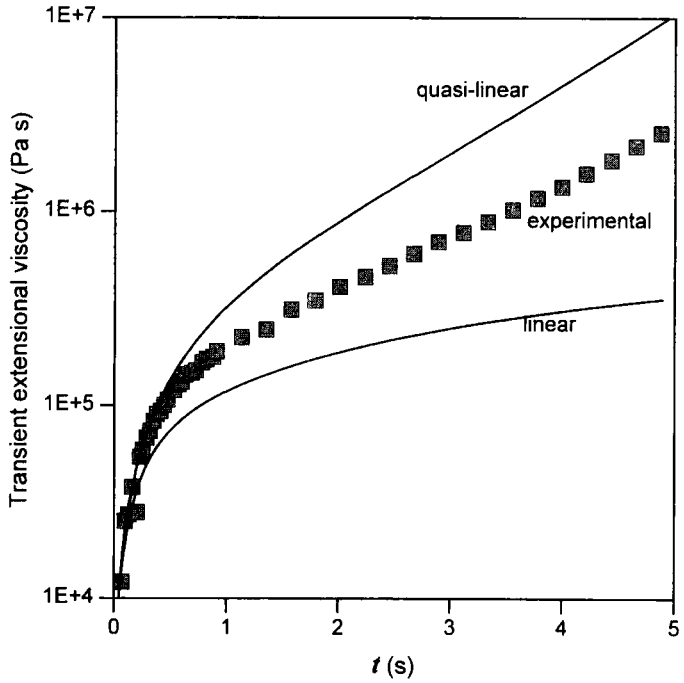

FIGURE 8 Transient extensional viscosity, $\bar{\eta}_E^+$, of M2 measured at a strain rate $\dot{\varepsilon}_0 = 0.51\,s^{-1}$ at 23°C. The experimental data are compared with theoretical predictions based on the discrete relaxation spectrum represented by solid lines in Figure 3.

Due to experimental scatter of the transient extensional viscosity data for A3 additional tensile tests were carried out in the load frame and simulated numerically with a single-mode, upper-convected Maxwell model whose parameters (viscosity, η, and time constant, λ) were fitted to the resulting stress-strain data [21]. Finally, the filament-stretching experiment was simulated with the use of this single-mode, quasi-linear model and the resulting curve for $\dot{\varepsilon}_0 = 2.4\,s^{-1}$ is labeled "quasi-linear (fitted)" in Figure 12. This model was used for the numerical simulations of the peeling process in Section 3.5 below.

For M3 the predictions of the transient extensional viscosity based on the LVE spectrum were significantly lower than the measured values, whereas for A3 the opposite was the case. On this basis, it can be concluded that the transient extensional viscosity outside the LVE

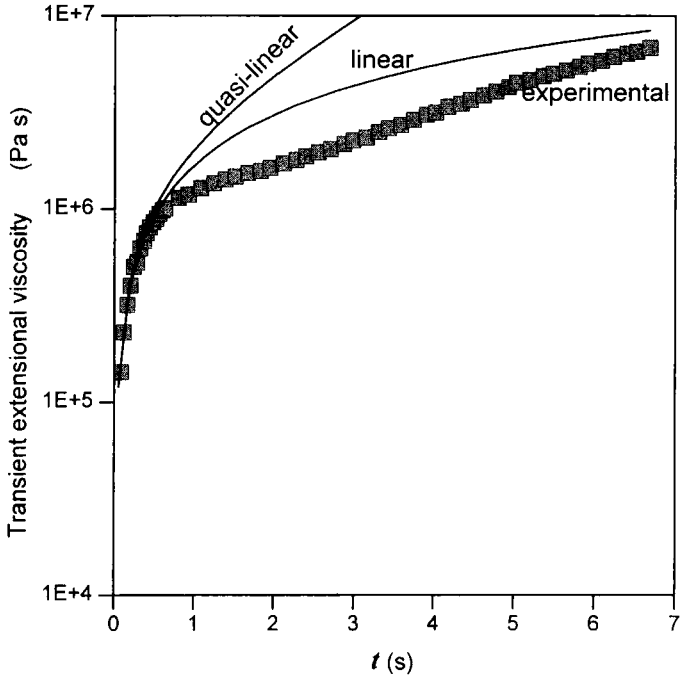

FIGURE 9 Transient extensional viscosity of A2 at $\dot{\varepsilon}_0 = 0.33\,s^{-1}$ at 23°C. The experimental data are compared with theoretical predictions based on the discrete relaxation spectrum represented by solid lines in Figure 4.

region may neither be quantitatively nor qualitatively correlated to the LVE properties for highly-crosslinked materials such as M3 and A3. The implication to adhesion is that the material response of highly-crosslinked PSA's to uniaxial elongation outside the LVE region may not be predicted from DMA data. Since the debonding step in peel and tack tests generally involves high extensional deformation of the adhesive, this should be kept in mind when establishing correlations between adhesive performance and rheology.

Given the above observations, the more general question arises: how can one know whether the large-strain, transient extensional response of a polymeric material may or may not be modeled on the basis of the available DMA data without having to spend the labour of doing extensional measurements? A method based on Eqs. (6) and (7) is proposed to answer this question.

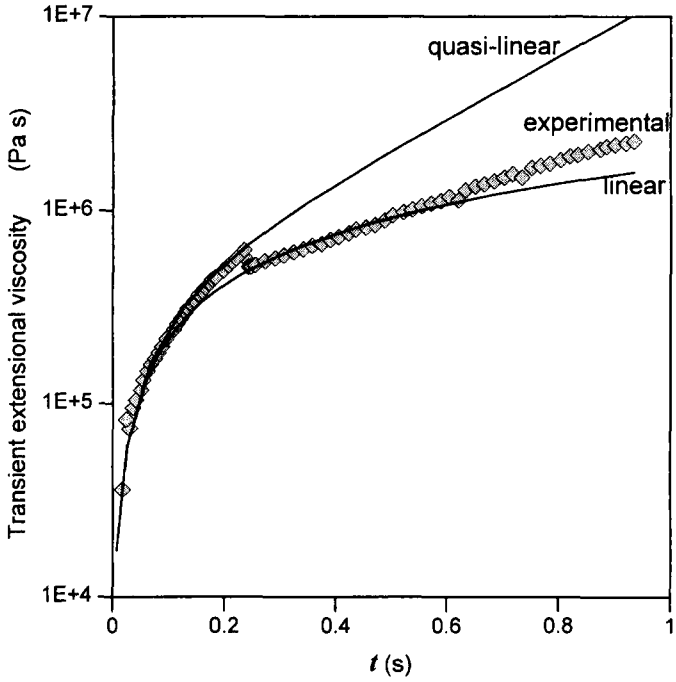

FIGURE 10 As Figure 9, but with $\dot{\varepsilon}_0 = 2.0\,s^{-1}$.

For the above tests the maximum experiment time, t_b, ranges from 1 to 7 seconds. On this basis, it is reasonable to include values of t up to 10 seconds in the following analysis. First, the *linear* model prediction of the stretching experiment of A1 is investigated more closely in Figure 13, where the contributions from individual relaxation modes to the total theoretical transient extensional viscosity according to Eq. (6) are given. The numbers indicated for each curve in the figure are the specific DMA test frequencies relating to the time constants in accordance with Eq. (7). At the very earliest times, the high frequency modes (low-time-constant modes) dominate the response but very soon the intermediate frequency modes gain more importance, whereas the low frequency modes (high-time-constant modes) gain only little importance within the given time frame. In the following, only three discrete values of $t = 0.1$, 1, and 10 seconds, indicated by vertical lines in Figure 13, are considered.

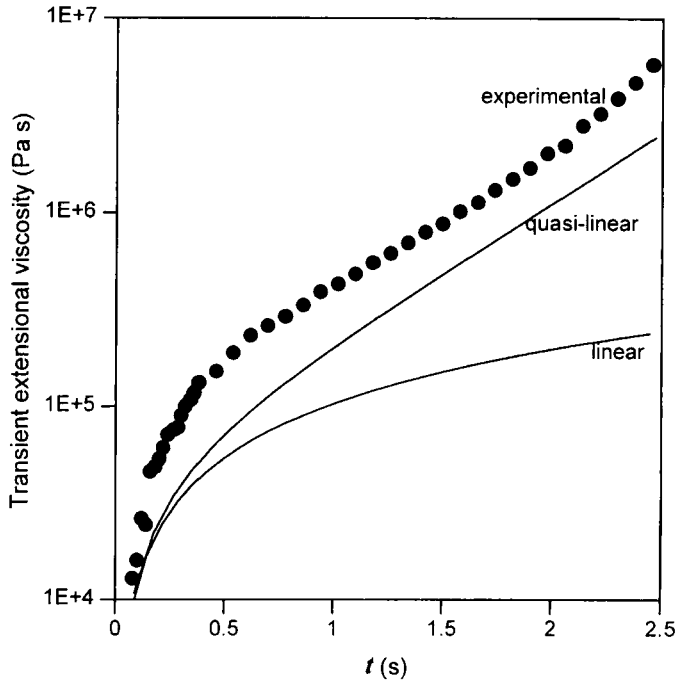

FIGURE 11 Transient extensional viscosity of M3 at $\dot{\varepsilon}_0 = 0.85\,s^{-1}$ at 23°C. The experimental data are compared with theoretical predictions based on the discrete relaxation spectrum represented by solid lines in Figure 5.

Figure 14 shows bar charts of f_i *versus* ω_i for each PSA in accordance with Eqs. (6) and (7) for the three values of t. The spectra of f_i for A1 in Figure 14(a) show what was already observed in Figure 13: a broad range of DMA test frequencies (corresponding to a broad range of time constants) are required to describe the transient extensional response of A1 over the two decades of t examined. It is noted that the intermediate frequency response is more critical, whereas the very high and the very low frequency response have little relevance, further indicating that the range of frequencies probed has provided sufficient information for defining the lower and the upper bound on the transient extensional viscosity given by the linear and quasi-linear models, respectively. This is verified by the fact that the measured transient extensional viscosity of A1 stays within these bounds at all times during the experiment, as seen in Figure 7. It

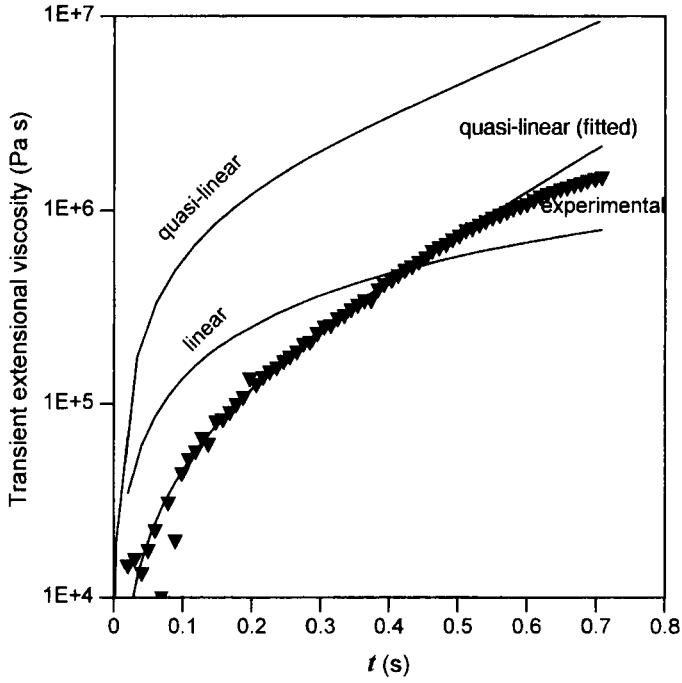

FIGURE 12 Transient extensional viscosity of A3 at $\dot{\varepsilon}_0 = 2.4\,s^{-1}$ at 23°C. The experimental data are compared with theoretical predictions based on the discrete relaxation spectrum represented by solid lines in Figure 6.

is emphasized that the spectra of f_i do not provide information about the strain-hardening characteristics of the material; such information can only be obtained in large-strain uniaxial elongational tests. The spectra of f_i for M2 and A2 in Figures 14(b) and (c) show the same overall trend as was observed for M2 above, with the addition of hydrocolloids shifting the spectra slightly towards lower frequencies. On this basis, the measured transient extensional viscosity of M2 and A2 is expected to remain within the bounds given by the linear and quasi-linear models which is verified for M2 in Figure 8 and partially verified for A2 in Figures 9 and 10. In contrast, the spectra of f_i for the crosslinked systems M3 and A3 in Figures 14(d) and (e) predict the very lowest frequencies probed to be by far the most important. This is a strong indication that the DMA data obtained have not provided the necessary information for predicting the transient extensional response

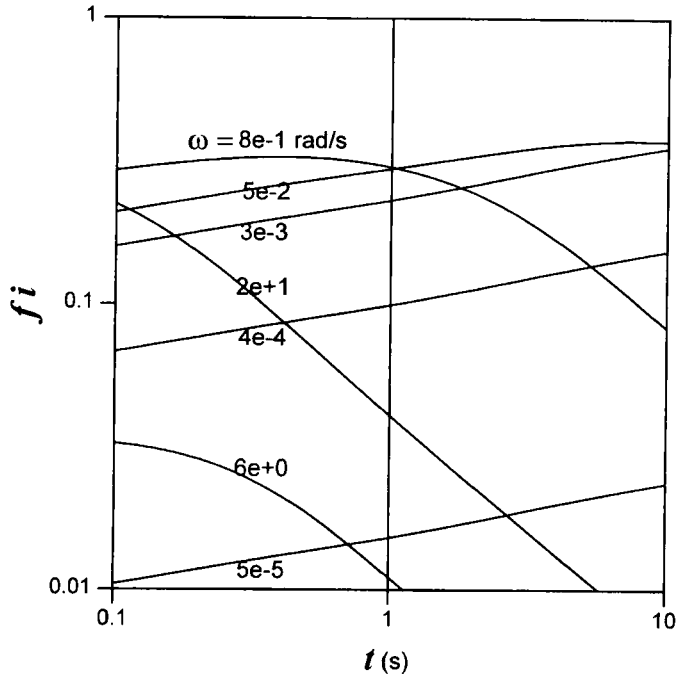

FIGURE 13 Fractional contribution, f_i, to the total transient extensional viscosity, $\bar{\eta}_E^+(t)$, from relaxation mode i according to Eq. (6) for adhesive A1. The number indicated for each curve is the specific DMA test frequency, $\omega_i = \lambda_i^{-1}$.

of these two PSA's; this is verified in Figures 11 and 12. The spectra of f_i for M3 and A3 suggest that DMA test frequencies, $\omega < 10^{-5}$ rad/s, should be probed in order to obtain a full description of the LVE properties. However, since $\omega = 10^{-5}$ rad/s is already quite a low test frequency, the results for M3 and A3 indicate that the transient extensional response of these two materials may not be modeled on the basis of their LVE spectra. This is probably the case for all polymers crosslinked beyond the gel point.

The above examples demonstrate how Eqs. (6) and (7) can be used to evaluate the likelihood of correlating the transient extensional viscosity of a polymeric material to the available DMA data. On this basis a criterion is proposed: If the discrete spectra of f_i obtained in accordance with Eqs. (6) and (7) predict high values of f_i at intermediate values of ω_i and decreasing values towards the highest and

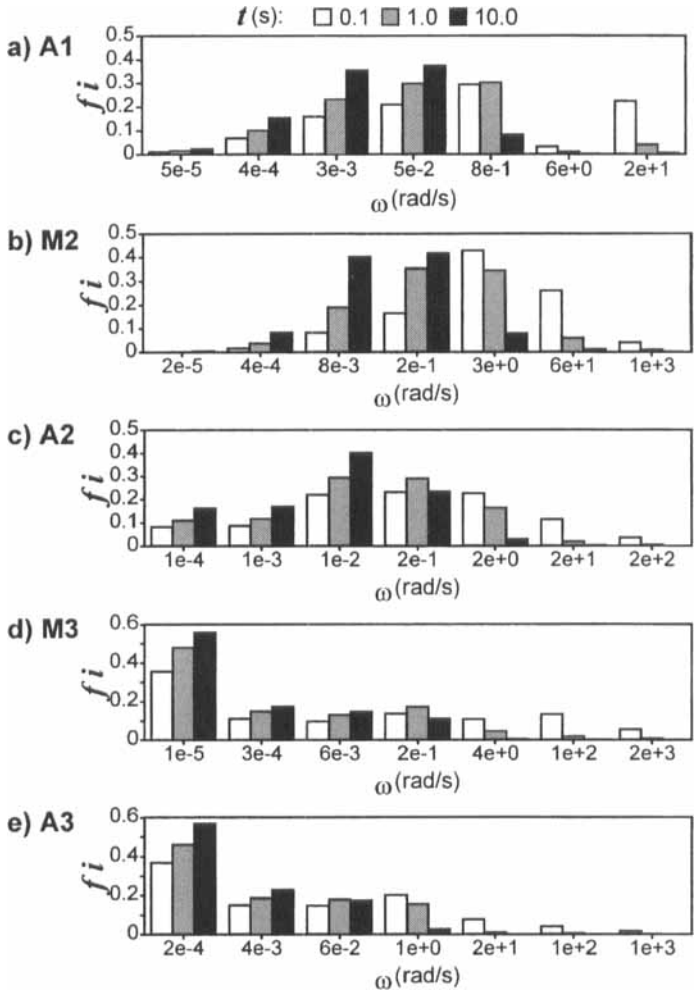

FIGURE 14 Spectra of f_i according to Eq. (6) at three values of t_b for (a) A1, (b) M2, (c) A2, (d) M3, and (e) A3. Each mode is represented on the *abscissa* by the specific DMA test frequency, $\omega_i = \lambda_i^{-1}$, where λ_i is the time constant of relaxation mode i.

lowest values of ω_i, the available DMA data will provide a lower and an upper bound for the transient extensional viscosity. On the other hand, if the largest value of f_i is obtained at the highest or lowest value of ω_i the DMA data obtained are insufficient for determining such bounds.

An exception to this rule is when the DMA data have provided information about the highest time constant mode of the material as indicated by a distinct plateau in the complex viscosity at the lowest frequencies, in which case the DMA data may still provide valid bounds for the transient extensional viscosity even if f_i attains its maximum at the lowest value of ω_i.

3.3. Observations of Peeling

For each peel test the average peel force over the length of the peeled adhesive was computed. The peel force values, F, given in Table II are mean values of three such averages. Also tabulated is the standard deviation (S.D.) of the three averages. Clearly, the relation between surface properties and peel force is ambiguous. However, the following trends can be recognized in Table II: (1) The peel force decreases with increasing surface roughness, and (2) A3 exhibits lower peel force than do A1 and A2.

Figure 15 shows images of A1, A2 and A3 being peeled from smooth substrates. For A2 and A3 the reflections clearly indicate how the adhesive is elongated in the peel front and that the deformation involves all of the adhesive from the substrate surface to the backing tape. It is further apparent that A2 is elongated much more than A3, corresponding to a considerably higher peel force. The difference in

TABLE II Average peel force values

Adhesive:	*A1*		*A2*		*A3*	
Substrate	*F (N)*	*S.D.*	*F (N)*	*S.D.*	*F (N)*	*S.D.*
PC-0	2.3	0.1	*c*[a]	–	1.5	0.3
PC-2	1.6	0.2	*c*	–	0.9	0.1
PC-8	1.7	0.1	*c*	–	0.8	0.0
PVDF-0	2.7	0.2	4.0	0.4	1.0	0.1
PVDF-3	2.5	0.2	2.4[b]	0.1	0.9	0.2
PVDF-9	1.4	0.4	2.0	0.3	0.7	0.1
SS-0	1.3	0.2	*c*	–	1.3	0.1
SS-4	4.4	0.3	*c*	–	1.6	0.1
SS-5	4.4	0.6	*c*	–	1.5	0.0
SS-7	4.1	0.0	*c*	–	1.3	0.2

[a] *c* = cohesive failure.
[b] one sample was excluded.

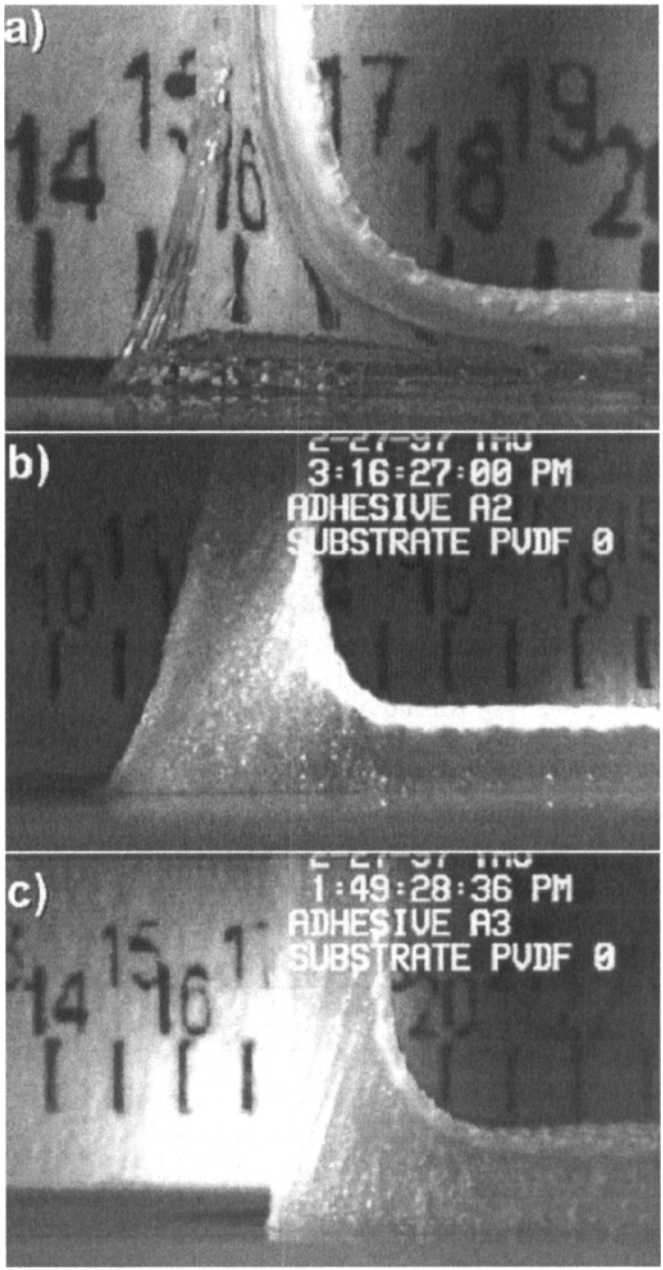

FIGURE 15 Peeling of (a) A1 from smooth PC, (b) A2 from smooth PVDF, and (c) A3 from smooth PVDF at peel rate, $v = 304$ mm/min. and 23°C.

rheology of the two adhesives offers two possible explanations for the difference in adhesive performance based on each of the two basic processes imparting adhesion: bonding and debonding.

The moduli of A2 decrease rapidly at decreasing frequency as characteristic of non-crosslinked polymeric fluids, and this adhesive will flow and wet even the roughest substrates during the bonding step and possibly diffuse into the surface of the substrate. In contrast, the moduli of M3 level out at the lowest frequencies, indicating that at 23°C A3 behaves as an elastic solid at slow deformations. This is probably so at temperatures below the glass transition temperature of the polystyrene-rich domains, $T_g \cong 80°C$ which constitute the physical cross-links. Thus, A3 may not be able to wet or diffuse completely into the substrate even after 24 hours at 60°C. The resulting reduction in true interfacial area or lack of interdiffusion would result in detachment from the substrate at a lower boundary stress during peeling as compared with A2. Apart from rheology, the strength of the interface between an adhesive and a substrate depends on the chemical compositions of both. Thus, the difference in chemistry of A2 and A3 may also be a source of the observed difference in peel force.

The second explanation for the difference in peel performance has to do with the debonding step with respect to the transient extensional properties of the adhesives and can be understood by comparing Figures 10 and 12. At early times, the transient extensional viscosity of A2 increases much faster than the transient extensional viscosity of A3, whereas, at later times, the opposite is the case. The implication for peeling is that at low values of x (corresponding to low values of t) the contribution from $\sigma(x)$ to P in Eq. (3) is significantly higher for A2 than for A3. This results in a higher peel force for A2 compared with A3 in cases of adhesive failure and high boundary stresses, even if the boundary stresses for the two adhesives were the same. However, the numerical simulations discussed in Section 3.5 below show that the boundary stress for A2 is substantially higher than for A3 at the same peel test conditions, which amplifies the effect.

In the images of the peeling of A1 and A2 in Figures 15(a) and (b) the length of the peel front, x_b, is seen to be between 4 and 5 mm, which corresponds to $t_b \cong 1$ second. Thus, according to Figures 14(a) and (c) a wide range of test frequencies is relevant for correlating the

LVE properties to the peeling process for A1 and A2, especially frequencies, ω, of the order 0.01 – 1 rad/s.

3.4. Reassessing the Dahlquist Criterion

The most famous statement regarding the correlation of viscoelastic properties and adhesive performance of PSA's was given by Dahlquist in 1966 [22]. Based on characterization of the rheological and adhesive properties of numerous commercial PSA's, he stated that in order for a PSA to wet a substrate properly during the short time of contact characteristic of a tack test the one second compressive creep compliance at the use temperature must be greater than 10^{-7} cm^2/dyne and preferably as high as 10^{-6} cm^2/dyne. However, the Dahlquist criterion is rarely quoted in its original form, but is reformulated in terms of oscillatory shear data (DMA data). In this form the criterion states that the absolute value of the complex shear modulus, $|G^*| = (G'^2 + G''^2)^{1/2}$, measured at 1 rad/s should not exceed $3.3 \cdot 10^5$ Pa and should preferably be as low as $3.3 \cdot 10^4$ Pa. This transformation of compressive compliance to complex shear modulus is based on the assumption that the viscosity ratio, $\eta_E(t)/|\eta*(\omega)| = 3$, where η_E is the extensional viscosity, η^* is the complex shear viscosity, and $\omega = 1/t$ For convenience, the contribution from G'' to $|G^*|$ is often neglected, and the Dahlquist criterion is then expressed in terms of G'. Since G' is typically greater than G'' or at least of the same order of magnitude at typical use temperatures, and since the Dahlquist criterion is only a rule of thumb, this is probably a reasonable simplification which leads to a simplified criterion stating that G'(1 rad/s) should be less than $3.3 \cdot 10^5$ Pa. This value is sometimes rounded off leading to an even simpler and easier to remember rule of thumb which states that G'(1 rad/s) should be below 10^5 Pa, and this is often referred to as the Dahlquist criterion, though it is rather different from the original statement.

As mentioned above, Dahlquist interpreted the criterion in terms of bonding, and this has been generally accepted since. It is important to note that in a tack test the quality of the bond formed between substrate and adhesive is never measured directly, but rather evaluated by measuring the force required to break the bond. Thus, the ability of the adhesive to resist debonding always influences the

measure of the quality of the bond. This allows for an alternative interpretation of the role of the one-second compressive creep compliance as it relates to the debonding step: In order for the adhesive to resist debonding it must be capable of dissipating a sufficient amount of energy before it detaches from the substrate. This places an upper bound on the tensile modulus, E, or in Dahlquist terms, a lower bound on the compressive creep compliance. Apparently, this interpretation of the Dahlquist criterion has not been considered previously, probably because the debonding step is generally believed to relate to the linear viscoelastic properties evaluated at higher frequencies. This belief is contradicted in the present work, and the idea that the Dahlquist criterion also relates to the debonding step is a consequence of this recognition.

3.5. Prediction of Peel Force

For each adhesive-substrate pair tested, two or more images of the peel front were analysed. From this analysis, the length of the peel front, x_b, and the apparent adhesive Hencky strain at detachment, $E_b = \ln(L_b/L_0)$, were derived. For each set of x_b and E_b the relevant rheological model was solved for the stress distribution, $\sigma(x)$, by assuming a parabolic strain rate profile [20],

$$\dot{\varepsilon}(t) = (4E_b t_b^{-2})t - (3E_b t_b^{-3})t^2, \quad 0 \leq t \leq t_b \tag{8}$$

Theoretical peel force values were then computed from the integral (3). The predicted and measured peel force values are compared for all adhesives and substrates in Figure 16. The non-linear model for A1, which did an excellent job at predicting peel forces in [20], tends to underpredict the peel force here, possibly because the actual contact area was increased as the 2 kg roll squeezed the unfilled adhesive while passing over it. Nonetheless, the main bulk of data points lie close to the diagonal, demonstrating the validity of the assumption of uniaxial deformation. Thus, the criterion proposed in Section 3.2 above for whether the transient extensional viscosity of a polymeric material can be modeled on the basis of the available DMA data also applies to the peeling of PSA's.

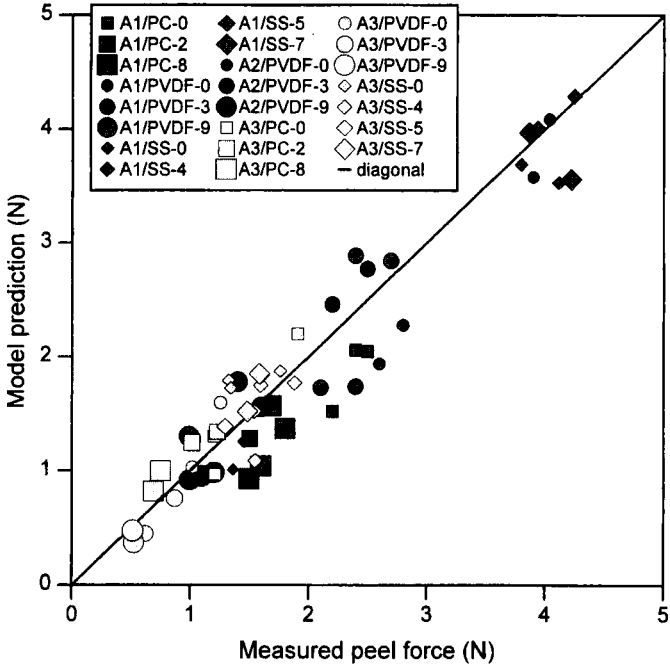

FIGURE 16 Peeling of A1, A2, and A3 from various substrates. The measured values of the peel force are plotted against the theoretical predictions based on the non-linear model for A1, the linear model for A2 and the single-mode, quasi-linear model for A3. Each data point refers to a single image of the peel front and the corresponding peel force reading. A quantitative predictive capability corresponds to the diagonal which is indicated by the solid line.

4. CONCLUSION

A criterion for whether the transient extensional viscosity of a polymeric material may be modeled on the basis of the linear viscoelastic spectrum measured in oscillatory shear has been proposed and evaluated experimentally for non-crosslinked as well as cross-linked pressure sensitive adhesives (PSA's). According to the criterion, the oscillatory shear data for the non-crosslinked PSA's provide an upper and a lower bound for the transient extensional viscosity, and this is verified experimentally. Furthermore, it is demonstrated that oscillatory shear data measured over a wide range of test frequencies are required in order to model accurately the transient extensional

response. When the criterion is applied to the crosslinked PSA's it becomes clear that oscillatory shear data do not provide the information necessary to model the transient extensional response, which is likewise in agreement with measured results. For such materials, the transient extensional properties must be measured independently in an extensional rheometer or a conventional load frame. Finally, peel tests were carried out and the deformation of adhesive was numerically simulated on the basis of images of the peel front and the assumption of uniaxial elongation. Excellent agreement between the resulting theoretical and experimental peel force values verifies the assumption of uniaxial elongation of adhesive during peeling and demonstrates the applicability of the criterion to the peeling process. For non-crosslinked PSA's this implies that a wide oscillatory shear test frequency range is relevant for correlating rheology and adhesive performance, whereas, for highly crosslinked PSA's, the linear viscoelastic spectrum mainly serves as a fingerprint of the adhesive composition.

Acknowledgements

O. Hassager (Technical University of Denmark), H. Everland (Coloplast Research), K. Almdal (Risø National Laboratory), and G. H. McKinley (Massachusetts Institute of Technology) are acknowledged for supervision throughout the Ph.D. project, *Rheology of Adhesion*. Dr. Stephen Spiegelberg (Massachusetts Institute of Technology) is acknowledged for extensive help in the laboratory. The project was funded by Coloplast A/S and the Danish Polymer Center.

References

[1] Gent, A. N. and Petrich, R. P., *Proc. R. Soc.* **A310**, 433 (1969).
[2] Verdier, C., Piau, J. and Benyahia, L., *C. R. Acad Sci. Paris* **323**, IIb, 739 (1996).
[3] Piau, J., Verdier, C. and Benyahia, L., *Rheol. Acta* **36**(4), 449 (1997).
[4] Connelly, R. W., Parsons, W. F. and Pearson, G. H., *J. Rheology* **25**(3), 315 (1981).
[5] Gupta, R. K., *J. Rheology* **27**(2), 171 (1983).
[6] Christensen, S. F., Everland, H., Hassager, O. and Almdal, K., *Int. J. Adhesion Adhesives* **18**, 131 (1998).
[7] Gent, A. N. and Hamed, G. R., *Polym. Eng. Sci.* **17**, 462 (1977).
[8] Gent, A. N. and Hamed, G. R., *Plast. Rubber: Mater. and Appl.* **3**(1), 17 (1978).
[9] Hamed, G. R., *Rubber Chem. Tech.* **54**, 403 (1981).

[10] Hamed, G. R., In: *Treatise on Adhesion and Adhesives* Vol. 6, Patrick, R. L., Ed. (Marcel Dekker, New York, 1989), Chap. 2.
[11] Satas, D. (1995). In: *Advances in Pressure Sensitive Adhesive Technology-2*, Satas, D., Ed. Satats and Associates, Warwick, Rhode Island, (1995), Chap. 1.
[12] Chang, E. P., *J. Adhesion* **60**, 233 (1997).
[13] Rohn, C. L., In: *Advances in Pressure Sensitive Adhesive Technology-2*, Satas, D., Ed., (Satas and Associates, Warwick, Rhode Island, (1995), Chap. 2.
[14] Wong, T. K. M., *Ph.D. Thesis* C.N.A.A. (1970).
[15] Tse, M. F., *Adhesives Age* September, p. 32 (1988).
[16] Tse, M. F., *J. Adhesion Sci. Technol.* **3**(7), 551 (1989).
[17] Tse, M. F., *PSTC Technical Seminar XVI*, Illinois May 5–7 (1993).
[18] Dale, W. C., Paster, M. D. and Haynes, J. K., In: *Advances in Pressure Sensitive Adhesive Technology-2*, Satas, D., Ed. (Satas and Associates, Warwick, Rhode Island, 1995), Chap. 4.
[19] Williams, M. L., Landel, R. F. and Ferry, J. D., *J. Am. Chem. Soc.* **77**, 3701 (1995).
[20] Christensen, S. F., McKinley, G. H., *Int. J. Adhesion Adhesives* **18**, 333 (1998).
[21] Christensen, S. F., *Rheology of Adhesion*, *Ph.D. Thesis* Technical University of Denmark (1998).
[22] Dahlquist, C. A., *Proc. Nottingham Conf. on Adhesion*, Part III (Maclaren & Sons Ltd., London, 1996), Chap. 5.

APPENDIX[1]

A1. Forms of Tensors in the Case of Time Varying Uniaxial Elongational Flow at Strain Rate, $\dot{\varepsilon}(t)$

Rate of strain tensor:

$$\dot{\gamma} = \begin{bmatrix} -1 & 0 & 0 \\ 0 & -1 & 0 \\ 0 & 0 & 2 \end{bmatrix} \dot{\varepsilon} \tag{A1}$$

Stress tensor:

$$\tau = \begin{bmatrix} \tau_{xx} & 0 & 0 \\ 0 & \tau_{yy} & 0 \\ 0 & 0 & \tau_{zz} \end{bmatrix} \tag{A2}$$

Upper convected time derivative of the stress tensor:

$$\tau_{(1)} = \frac{\partial}{\partial t} \begin{bmatrix} \tau_{xx} & 0 & 0 \\ 0 & \tau_{yy} & 0 \\ 0 & 0 & \tau_{zz} \end{bmatrix} - \begin{bmatrix} -\tau_{xx} & 0 & 0 \\ 0 & -\tau_{yy} & 0 \\ 0 & 0 & 2\tau_{zz} \end{bmatrix} \dot{\varepsilon} \tag{A3}$$

[1]Bird, R. B., Armstrong, R. C. and Hassager, O., *Dynamics of polymeric liquids*, vol. 1 (John Wiley & Sons, Inc. USA, 1987).

A2. Transient Extensional Viscosity

$$\bar{\eta}_E^+ \equiv -\frac{\tau_{zz} - \tau_{xx}}{\dot{\varepsilon}} \tag{A4}$$

A3. Constitutive Equations

Linear model (Generalized linear Maxwell model, solvent term omitted):

$$\tau_i + \lambda_i d\tau_i/dt = -\eta_i\dot{\gamma}, \quad i = 1, 2, \ldots, N \tag{A5}$$

$$\tau = \sum_{i=1}^{N} \tau_i \tag{A6}$$

Quasi-linear model (Generalized upper convected Maxwell model, solvent term omitted):

$$\tau_i + \lambda_i \tau_{(1),i} = -\eta_i\dot{\gamma}, \quad i = 1, 2, \ldots, N \tag{A7}$$

$$\tau = \sum_{i=1}^{N} \tau_i \tag{A6}$$

Non-linear model (Generalized Giesekus, solvent term omitted):

$$\tau_i + \lambda_i \tau_{(1),i} - \alpha_i \frac{\lambda_i}{\eta_i}(\tau_i \cdot \tau_i) = -\eta_i\dot{\gamma}, \quad i = 1, 2, \ldots, N \tag{A8}$$

$$\tau = \sum_{i=1}^{N} \tau_i \tag{A6}$$